PERFORMANCE OF WOOD PLASTIC COMPOSITE FOUNDATION ELEMENTS IN POST-FRAME AND LIGHT-FRAME SHEAR WALLS

By

LOREN ALLEN ROSS

A thesis submitted in partial fulfillment of
the requirements for the degree of

MASTER OF SCIENCE IN CIVIL ENGINEERING

WASHINGTON STATE UNIVERSITY
Department of Civil and Environmental Engineering

AUGUST 2008

To the Faculty of Washington State University:

The members of the Committee appointed to examine the thesis of LOREN ALLEN ROSS find it satisfactory and recommend that it be accepted.

_____

Chair

_____

_____

ACKNOWLEDGEMENTS

I need to thank many people for their support and assistance with my research, but I cannot imagine that I would have ever finished without the following people:

- My wife, Katy, is always my support and without her, I'm not sure if I would ever get anything done. She read my thesis many times even when it was boring, and she was tired.
- Dr. Bender for getting me to WSU in the first place and for supporting me along the way in whatever came up, also for letting me be in charge sometimes.
- Dr. Dolan for always being available for technical know-how and for being a great example of a great guy in and outside the classroom.
- Dr. Pollock for making me aware that WSU existed and always being kind.
- Rich Utzman for helping me melt, lift, build, test, and destroy materials and walls that I could not have done without his help. Also for adding a sense of calm, wisdom, and perspective to my hectic project. I wish I could help him as much as he has helped me.
- Trex and Spokane Structures for donating material and technical information.
- The Office of Naval Research, under the direction of Mr. Ignacio Perez, for providing Grant N00014-06-1-0847 which allowed this work to even start.

PERFORMANCE OF WOOD PLASTIC COMPOSITE FOUNDATION ELEMENTS IN POST-FRAME AND LIGHT-FRAME SHEAR WALLS

Abstract

Loren Allen Ross, M.S.
Washington State University
May 2008

Chair: Donald A. Bender

The resistance of lateral loads in either post-frame or light frame structures typically depends upon diaphragm action and shear walls. Shear walls also have the added challenge of being in contact with the ground and concrete, which requires special protection to prevent decay in wood components. Often, these foundations elements suffer environmental deterioration, which consequently compromises the lateral resisting system. Also, there is growing concern that preservative chemicals used to treat lumber have adverse environmental impacts. Similarly, the copper-rich preservative treatments cause corrosion of the fasteners, which can compromise the structure.

One possible solution is to replace treated lumber with wood plastic composites (WPC) as foundation elements. WPCs lack the chemical treatments found in preservative pressure treated (PPT) lumber, yet they can resist decay and insect attack. Unfortunately, WPC are currently not used for many structural applications because of a lack of test data on its performance.

This thesis presents the use of WPCs as foundation elements in both a post-frame wall and a light-frame wall. Strength and stiffness of walls with WPCs are compared to walls with PPT lumber foundation elements to investigate possible substitution options.

TABLE OF CONTENTS

LIST OF FIGURES

LIST OF TABLES

CHAPTER 1

Introduction

This research was conducted to examine the feasibility of substituting wood-plastic composites (WPC) for preservative pressure treated (PPT) lumber in foundation elements. Previously, Duchateau (2005) tested a direct substitution of a WPC sill plate for PPT lumber in light-frame walls. She also tested a more economical “three box” hollow section and a thicker section WPC that allowed studs to be inserted into the sill plate and steel rods to be used as holdowns. The research presented in this thesis builds on Duchateau’s work by exploring the use of WPC for skirtboards in post-frame buildings and the use of alternative holdown methods in light-frame walls.

Post-frame buildings use PPT lumber for the skirtboard or bottom girt of the wall. The skirtboard is in contact with moisture from the ground and concrete floors. Skirtboards also act as a necessary part of the lateral force resisting system by acting as a collector strut for the forces on the shear wall. In Chapter 2, the viability of substituting WPC skirtboards was tested by performing monotonic racking tests on walls with and without WPC skirtboards and two common types of wall construction. Strength and stiffness were compared to determine if a WPC skirtboard was statistically equivalent to a PPT skirtboard.

A study of two different alternatives of light-frame shear walls without PPT sill plates is presented in Chapter 3. The walls underwent reverse cyclic loading to find strength and stiffness values of the alternatives. They are then compared to walls without holdowns using a PPT sill plate to determine their performance.

CHAPTER 2

Performance of Post-Frame Shear Walls with a Wood Plastic Composite Skirtboard Subjected to Monotonic Racking Loads

ABSTRACT

Shear walls in post-frame buildings are typically constructed with timber posts and horizontally framed wall girts from dimension lumber. The bottom wall girt, called the skirtboard or splashboard, is typically preservative pressure treated (PPT) due its location near the ground. Consumer concerns over chromated copper arsenate (CCA) PPT lumber has led to new copper-rich chemical formulations that have the potential for accelerated corrosion of the steel panels and fasteners (Bohnhoff, 2002; Zelinka and Rammer, 2006). Concurrent with this shift in preservative chemicals, the wood-plastic composite (WPC) lumber industry has rapidly grown to a current level of one billion U.S. dollars in North America alone (Wolcott et al., 2006). Wood plastic composite lumber is an environmentally benign alternative to PPT lumber, but WPC products have different mechanical properties than lumber (Bender et al., 2006), so consideration must be given when substituting WPC products in structural PPT applications.

In this study a commercially available WPC product is used as a skirtboard in two common configurations of post-frame endwalls to evaluate changes in strength due to substituting PPT wood with a WPC. The study determines that two 3.8 cm by 14 cm WPC boards can be substituted for a single 3.8 cm by 24.1 cm PPT board without affecting the strength of the endwall.

INTRODUCTION

According to the National Frame Builders Association (NFBA), the post-frame industry was valued at between 10 and 11 billion U.S. dollars in 2002. Post-frame construction differs from traditional light-frame wood construction; instead of stud walls, post-frame buildings have

timber posts, usually spaced 1.83 m to 3.66 m apart, which directly support the roof. Wall girts are fastened across the posts to allow attachment of sheathing. There are two typical ways to fasten the girts to the posts. Dimension lumber can be mounted on the outside surface of the post in a flatwise orientation. This method, known as flat construction, requires minimal labor, yet it causes the girts to bend about their weak axis to resist transverse loads such as wind. Another method of construction, known as edgewise construction, is to inset the girts between the posts with the larger dimension parallel with the ground so that the girt is loaded edgewise. Blocking, toe-nailing, or proprietary fasteners are needed for the girt-to-post connection, which requires more material and labor than flat construction.

In either configuration, the bottom girt, called the skirtboard or splashboard, can be exposed to wet conditions because it is located near ground level. In addition, the skirtboard is often used as the formwork for casting a concrete floor inside the building.

Not only do skirtboards face significant environmental loadings, but they also act as an important component of the load path for post frame buildings. The skirtboard collects the forces from the sheathing and transfers it into the posts and foundation; thus, the durability of the environmentally attacked skirtboard is of structural importance.

The method of increasing the durability of wood changed significantly when the Environmental Protection Agency announced that arsenic would no longer be used in residential and non-industrial uses (Lebow et al., 2003). Instead of CCA,, alternatives with higher copper contents have gained market share such as alkaline copper quaternary (ACQ) and copper azole (CuAz). The down side to these copper-rich formulations is the increased galvanic corrosion of fasteners in the wood. While this voluntary phase-out of CCA does not have a direct effect upon agricultural and commercial post-frame construction, it has increased the difficulty in finding

CCA treated skirtboard material, and it has created a movement towards possibly eliminating CCA altogether (Bohnhoff, 2002).

One alternative to using copper-rich PPT lumber in post-frame buildings is to replace it with WPC material. This study assesses the feasibility of that option. Four 3.7m by 3.7 m wall configurations were built, half with a commercially available WPC skirtboard and the other half with a PPT lumber skirtboard. Each skirtboard configuration was also tested using flatwise and edgewise girt construction. All configurations were subjected to monotonic wall racking tests to evaluate their shear performance. The specific objective of this study was to determine possible influences of skirtboard material (PPT lumber vs. WPC) and girt orientation (flatwise vs. edgewise) on the following structural properties:

- peak and design lateral resistance strength
- displacement at maximum and design loads
- internal shear stiffness

MATERIALS AND METHODS

Materials

Two types of skirtboad materials were used. The control case was PPT, incised Hem-fir graded as No. 2 or better lumber of 3.8 cm by 24.1 cm dimensions. A commercial WPC made from a high density polyethylene formulation was chosen to represent the most common polymer currently available and one which has a relatively low modulus of elasticity compared to other polymer types such as polypropylene and polyvinyl chloride (Bender et al., 2006). Specifically, the WPC skirtboard was Trex Accents® with dimensions of 3.8 cm by 14 cm having design values given in Table 2.1. All non-treated lumber, used for wall girts and blocking, was

Douglas-fir graded as No. 2 or better and was either a 3.8 cm by 14 cm or 3.8 cm by 8.9 cm, depending on location within the wall. The posts were Hem-Fir graded as No. 2 or better with dimensions of 14 cm by 14 cm. The posts were incised and pressure-treated with CCA.

The fasteners for the walls were 20d (4.88x102 mm) bright, common for wood to wood connections. For a metal to wood connection, Fabral WoodFast 4x38.1 mm, galvanized screws were used. Similarly, Fabral WoodFast 4x25.4 mm screws were used for stitch screws which secure the overlapping metal sheets together. The metal was 29 gauge Delta Rib manufactured by Jenysis.

Wall Construction

Two factors were examined in this study: 1) PPT lumber vs. WPC and 2) edgewise vs. flat girt construction. The different wall configurations are shown in Figures 2.1 and 2.2. The posts for all configurations were 4 m long with a wall height of 3.7 m. The extra 0.3 m post length was used to attach the walls to the testing floor. Wall constructions and fixtures generally followed the methods given in the Braun Intertec (1996) report to the National Frame Builders Association.

For the edgewise girt orientations, interior girts were offset to be in the same plane as the flatwise mounted skirtboard and top girt. The blocking between girts was attached with two 20d common nails to the posts, and then two more nails were driven through the top of the girt into the blocking. To allow the metal sheathing to be attached around the edges of the walls, a 3.8 cm by 8.9 cm Douglas-fir graded as No. 2 or better board was attached to the face of the post. For the flatwise girts, two nails were driven through the face of the girt into the post on each side.

The 20d common nails were driven by hand with 3.6 mm diameter holes predrilled into the WPC. Eight nails were used for each side of the skirtboard. For the PPT skirtboards, 16 nails were driven into each side without predrilling because its lower density did not require it.

The Fabral screws were driven with a variable speed screwdriver. The screws were driven according to Fabral's instructions, which stated that the neoprene washer should not "mushroom" beyond the metal top of the washer (Fabral, 2000). For the stitch screws, overdriving was avoided by setting the clutch of the power drill used as a screwdriver. Overdrilling was prevented with the metal-to-wood connection screws by controlling the speed of the screwdriver.

Test Methods

Monotonic testes were performed according to ASTM E 564 (ASTM, 2006) and ASAE EP558 (ASAE, 2004). When the two standards conflicted, the method that was followed was carefully documented. For example, ASTM E 564 requires a preload of 10% of the ultimate load; whereas, ASAE EP588 only requires a 5% preload. The ASTM E 564 preload of 10% was followed. Similarly, ASAE EP558 requires that the ultimate load is reached "in not less than 10 minutes" versus the 5 minutes required by ASTM, so the ASAE method was followed.

The ASAE EP558 method of loading the wall at a constant rate of displacement was followed over the ASTM E 564 method of stepped incremental loads. The load rate was 6.35 mm/min and was calculated from Alumax's Powerpanel Test Data (Alumax, 1992) and two trial walls whose construction and testing were used for the calibration of the testing procedures. The load was applied uniformly across the top of the wall by attaching the top girt, which simulated a bottom chord of a truss, to a steel channel. The channel was attached by twelve, 6.35 x 51 mm

self-drilling screws spaced 30.5 cm apart and 15.25 cm from each end of the girt. A 445 kN rated hydraulic actuator was then attached to the steel channel to apply the force into the wall.

The posts were attached to the testing floor through pin-connections. While actual posts might have some moment-resisting capacity due to embedment, pin-connections were conservatively used in testing to require the skirtboards to resist more force. The pin-connections were created by sandwiching the posts between 6.35 mm metal plates. Four 1.59 cm diameter bolts attached the metal plates to the posts. On the other end of the plates, a single 2.54 cm diameter threaded bar was passed through the metal plates with a 10.2 by 10.2 cm metal square tube between the plates. This metal tube was then attached to the strong-floor with four 2.54 cm diameter bolts.

Since the walls were constructed and tested parallel with the ground, rollers were placed under the center of each girt to minimize deflection due to the self-weight of the wall. For the WPC skirtboards, two rollers were necessary since WPC has a lower modulus of elasticity than wood. Similarly, two rollers were placed under the steel channel so that its weight was not carried by the wall. Steel tubing was also place just above the steel channel to resist lateral deflection at the top of the wall. The steel tubing did not rest on the channel, and since significant buckling of the top chord never occurred during testing, they never made contact with the channel. A roller was also placed under each post to carry their self weight.

Deflection data were collected in four locations on the wall according to ASTM E 564 (ASTM, 2006). These locations were as follows:

1) Lateral displacement of the top of the wall
2) The uplift of the bottom corner of the wall on the side of the actuator
3) The crushing of the bottom corner of the wall opposite the actuator

4) The lateral slip at the bottom of the wall of the corner opposite the actuator.

All displacements were measured with linear potentiometers (string pots). Figure 2.3 shows a diagram of where the string pots were located

Moisture content of the wood members was taken with a resistance meter. The average moisture content for the posts was 30.5% and 9.6% for all other lumber.

RESULTS AND DISCUSSION

Twelve walls were tested with half using edgewise girt construction and the other half using flatwise girt construction. Also, half of the walls utilized PPT lumber skirtboards and the other half utilized WPC skirtboards. The nomenclature used for naming the walls was that the first letter represents if the wall was an edgewise (E) or a flat (F) construction. The second set of letters designates if the wall had a pressure-treated (PT) or WPC (WP) skirtboard. The ending number represents the iteration of that type of wall. For example EWP3 would be the third edgewise wall with a WPC skirtboard.

Definitions of Calculated Parameters

Walls subjected to monotonic tests undergo rigid body rotation and translation as well as shear displacement; however, it is only the shear displacement that is of interest. Rigid body translation was measured using string pot #4 on Figure 2.3. Rigid body rotation was a more difficult process. The values of string pots #2 and #3 were combined with the distance between string pots to provide the rigid body rotation. The distance between measurement points were 3.52 m and 3.72 m for the width and height, respectively. Figure 2.4 shows the various types of displacements experienced by wall EWP1.

As can be seen in Figure 2.4, the early displacement was caused by rotation and translation. These displacements occurred largely due to the crushing of the posts around the four bolts connecting the posts to the metal plates. There appeared to be minimal slippage of the metal fixtures before becoming engaged with the reaction floor.

Ultimate load for each specimen was taken as the maximum load the wall resisted during testing. The primary yield mode occurring at the maximum load was buckling of the sheathing. The tests were run well past the buckling load to guarantee that the peak load was reached. Usually the tests were run until the wall only resisted 90% of the maximum force measured. For clarity, all charts in this report stop at the maximum load of the wall.

Shear strengths of the twelve walls tested were considerably stronger than the walls tested in the Alumax (1992) study. Alumax's "Q-2" category of walls is closest to the walls tested in this study; however, their design strength for flatwise girt walls with pressure-treated skirtboards was 2.48 kN/m compared to 3.08 kN/m obtained in this study. Alumax's walls differed in two significant areas: post spacing and girt spacing. Alumax spaced posts 2.44 m on center (o.c.), which is a common spacing in the eastern United States. Posts in this study were spaced approximately 3.66 m o.c., which is a more common spacing for the western U.S. This difference, however, should have made Alumax's walls stronger. The second difference apparently had more impact on the strength. Alumax's walls had girts spaced at 0.91 m o.c.; whereas, the walls in this study had girt spacing of 0.61 m o.c. Since a primary failure mechanism of the walls was buckling of the metal sheathing, reducing the distance between girts significantly increased the buckling capacity.

Design shear strengths of the walls were found by taking the maximum load and dividing by the width of the wall (3.66 m) and by a safety factor of 2.5. The ASAE procedure of

averaging all three walls per configuration was used instead of the ASTM method of averaging the weakest two of the three walls. Table 1 shows the ultimate shear strength and design strength of each wall. The coefficients of variation (COV) calculated from three wall replications per configuration are given in Table 2.

Once the internal shear displacement and design load were calculated, the internal shear stiffness was determined. This value was calculated by dividing the design load by the internal shear displacement at that load, and then multiplying by the height-to-width ratio of the wall. This ratio was 1.0 for these walls. According to ASAE EP558, the stiffness value is found by averaging all three walls, not the weakest. Table 1 shows the average value for each configuration.

As Table 1 indicates, the internal shear displacement of all wall configurations was similar. A statistical ANOVA test was conducted and no significant differences were found between flatwise and edgewise girt orientations or between PPT and WPC skirtboards. Figures 2.5 through 2.8 show the load versus displacement plots for each wall organized by configuration.

An unexpected result of this study was that the COV of the WPC skirtboards was higher than that of the PPT skirtboards. This result was unexpected because WPC products are generally more homogeneous than wood and have a smaller COV for material properties. The most probable explanation for this apparently counterintuitive outcome was variability in how the test wall specimens were fabricated – i.e. two different laboratory technicians assembled the walls.

Failure Modes

The primary yield mode for the walls was the buckling of the metal sheathing, with failure being defined as the ultimate load. The buckling started between the second and third girt (including the skirtboard as a girt) from the bottom. This spot was the first gap between girts that spanned a full 0.61 m. Apparently, the decreased span of the metal between the skirtboard and the second girt increased the capacity of the metal enough that the next span became the weakest spot. The buckling created a crease along the space between the second and third girt and eventually created diagonal waves throughout the panel sheathing. The buckling occurred approximately 30° from the vertical.

The stitch screws and the screws attaching the metal to the girts were another failure mode for the tested specimens. The screws would either pull out of the wood or metal or the metal would tear around the screw. This failure mode did not occur in all walls, but would most frequently happen on the side of the wall opposite the actuator, which was undergoing compression. Once a screw failed, the buckling of the sheathing was affected as forces had to become redistributed around that failed section. It was observed that underdriving or overdriving the screws affected their performance, highlighting the need for correct and consistent attachment of the screws for optimal wall performance.

The skirtboards exhibited minimal buckling during the testing, with out-of-plane displacements less than 5 mm. They formed a full sine wave about their weak axis from post to post. The WPC skirtboard buckled the most, as would be expected with its lower modulus of elasticity; however, buckling of either type of skirtboard was slight and did not appear to affect wall behavior.

SUMMARY AND CONCLUSIONS

Monotonic shear wall tests were performed on four configurations of post-frame walls. Potential differences between a PPT lumber and a WPC skirtboard were investigated for both flatwise and edgewise wall girt constructions. Shear wall tests were performed according to ASTM E 564 (ASTM, 2006) and ASAE EP558 (ASAE, 2004) standards.

As shown in Table 2, values for WPC skirtboards were nearly equal to the values for pressure treated skirtboards. ANOVA testing found no statistically significant differences between flatwise and edgewise girt orientations or between PPT and WPC skirtboards. This result suggested that designers can substitute a 3.8 cm by 24.1 cm pressure-treated skirtboard for two 3.8 cm by 14 cm WPC boards without sacrificing the ultimate strength or stiffness of the walls. Hence, WPCs appear to be good materials to substitute for PPT lumber where copper-rich preservative chemical formulations could accelerate corrosion in the sheathing and fastening materials.

When comparing the strength of these walls with those tested in the Alumax study, the impact of girt spacing was shown to be a significant factor. By decreasing the spacing between girts, designers can expect a significant improvement to ultimate shear strength. The increased strength is due to the reduction of the span between supports of the metal which strengthens the metal against buckling.

Literature Cited

Alumax Building Products. 1992. Powerpanel test date for post-frame end walls with diaphragm loading. Alumax Building Products, Reidsvill, NC.

ASAE. 2004. EP558 Load tests for metal-clad wood-frame diaphragms. American Society of Agricultural and Biological Engineers. St. Joseph, MI.

ASTM Standards. 2006. E564-06 Standard practice for static load test for shear resistance of framed walls for buildings. West Conshohocken, PA: ASTM.

Bender, D.A., M.P. Wolcott and J.D. Dolan. 2006. Structural design and applications with wood-plastic composites. Wood Design Focus – A Journal of Contemporary Wood Engineering 16(3):13-15.

Bohnhoff, David R. (2002). Post Foundation design considerations. Wood Design Focus – A Journal of Contemporary Wood Engineering 12(3):10-16.

Braun Intertec. 1996. Load testing wood framed steel panel roof and end wall diaphragms. Report #05-106-1975 to the National Frame Builders Association, Lawrence, KS.

Fabral. 2000. Standard details for post-frame and residential structures. Technical brochure, Fabral Metal Wall and Roof Systems, Lancaster, PA.

Lebow, S., J. Winandy and D.A. Bender. 2003. Treated wood in transition – a look at CCA and candidates to replace it. Frame Building News 15(5):32-38.

Wolcott, M.P., P.M. Smith and K.R. Englund. 2006. Technology and market issues driving wood-plastic product development. Wood Design Focus – A Journal of Contemporary Wood Engineering 16(3):3-5.

Zelinka, S.L. and D.R. Rammer. 2006. Corrosion avoidance with new wood preservatives. Wood Design Focus – A Journal of Contemporary Wood Engineering 16(2):7-8.

LIST OF FIGURES

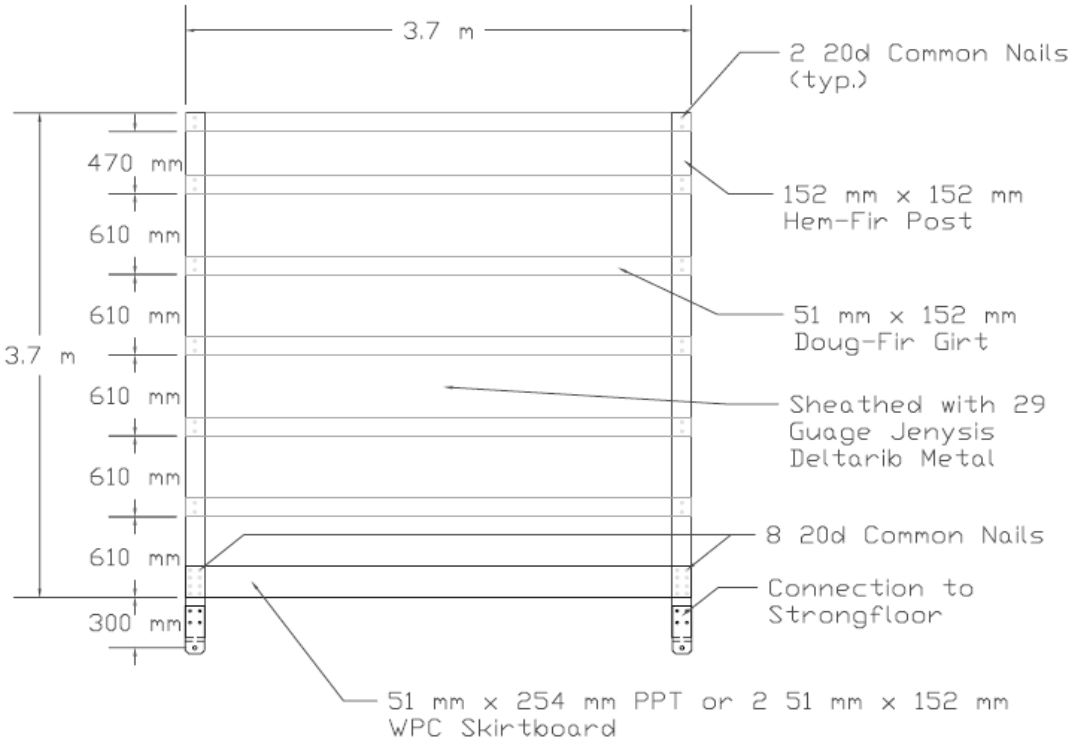

Figure 2.1 Flatwise wall girt orientation.

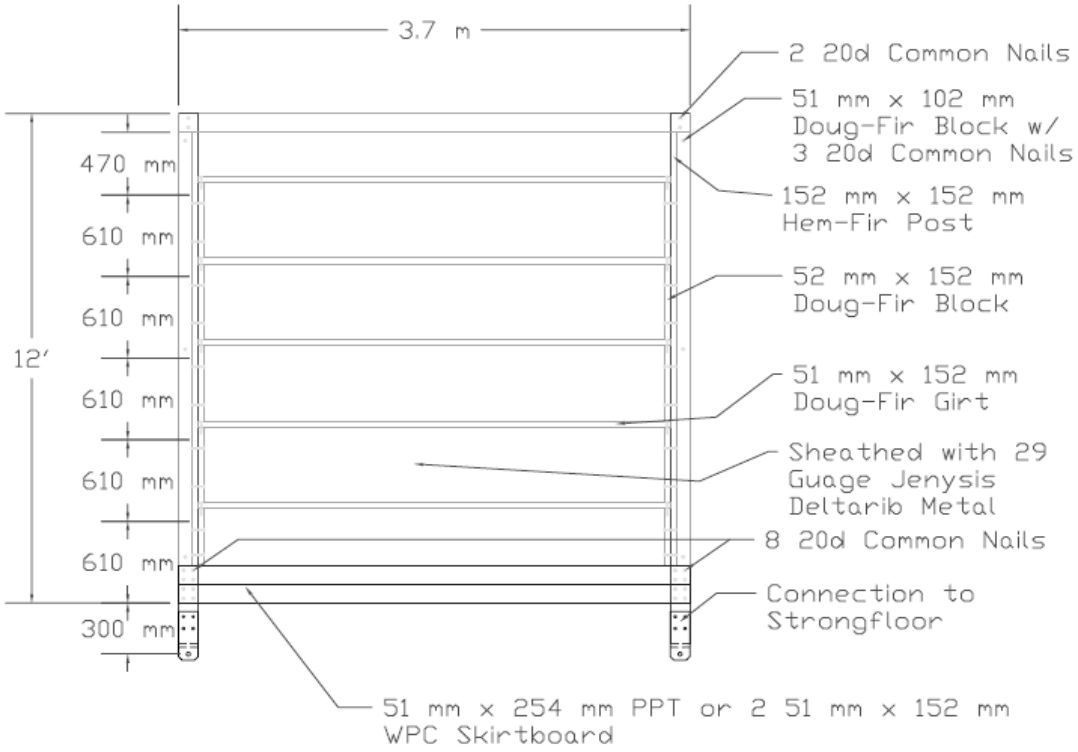

Figure 2.2 Edgewise wall girt orientation.

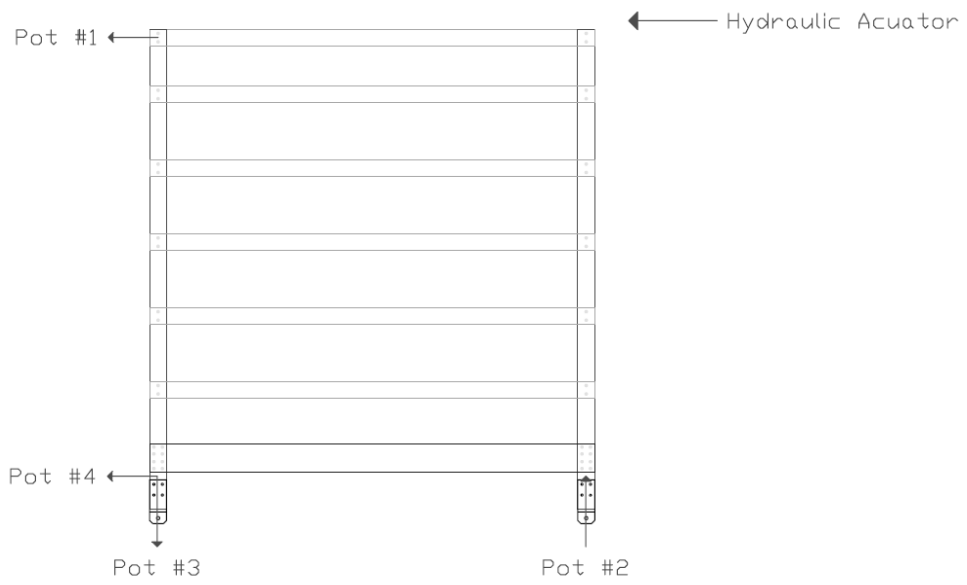

Figure 2.3 Location of string potentiometers to measure rigid body translation, rotation, and internal shear displacement.

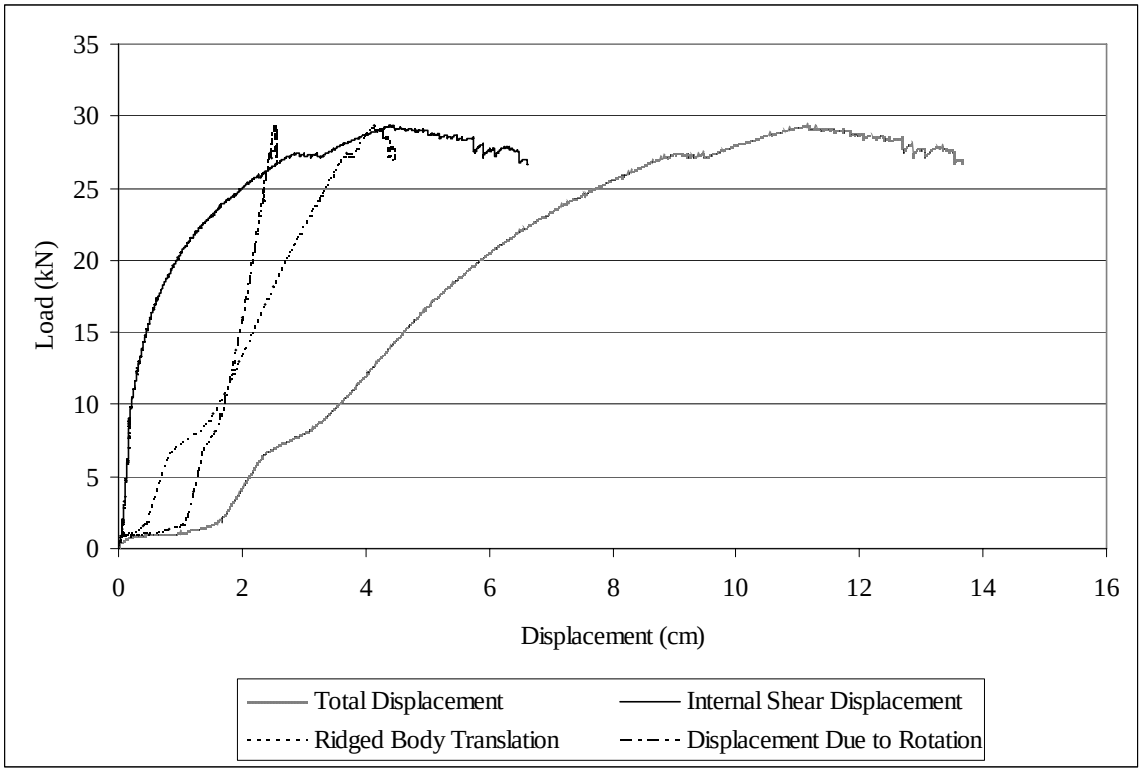

Figure 2.4 Displacements of a wall with edgewise girts and a WPC skirtboard.

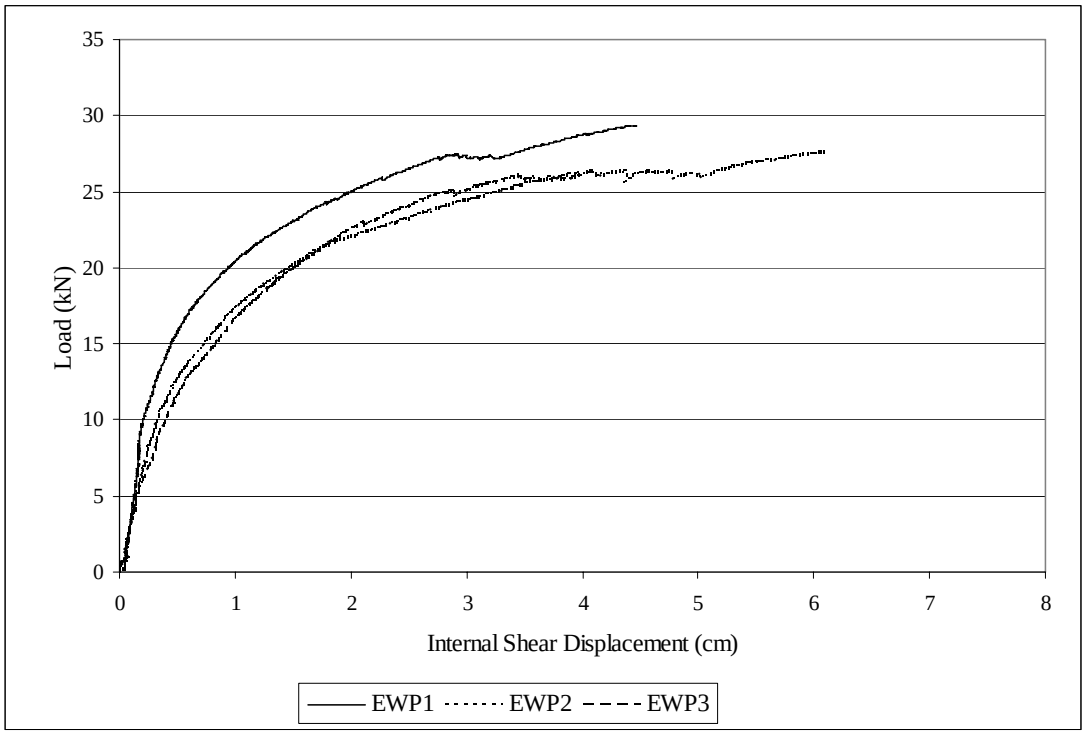

Figure 2.5 Internal shear displacements of walls with edgewise girts and WPC skirtboards.

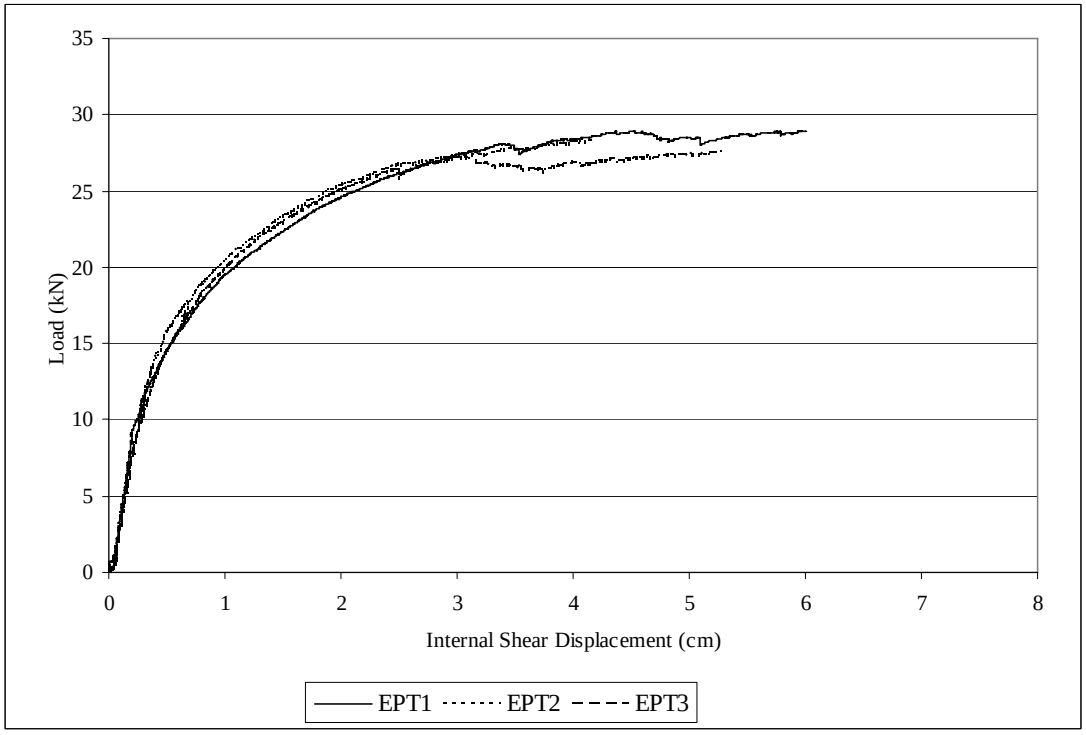

Figure 2.6 Internal shear displacements of walls with edgewise girts and PPT skirtboards.

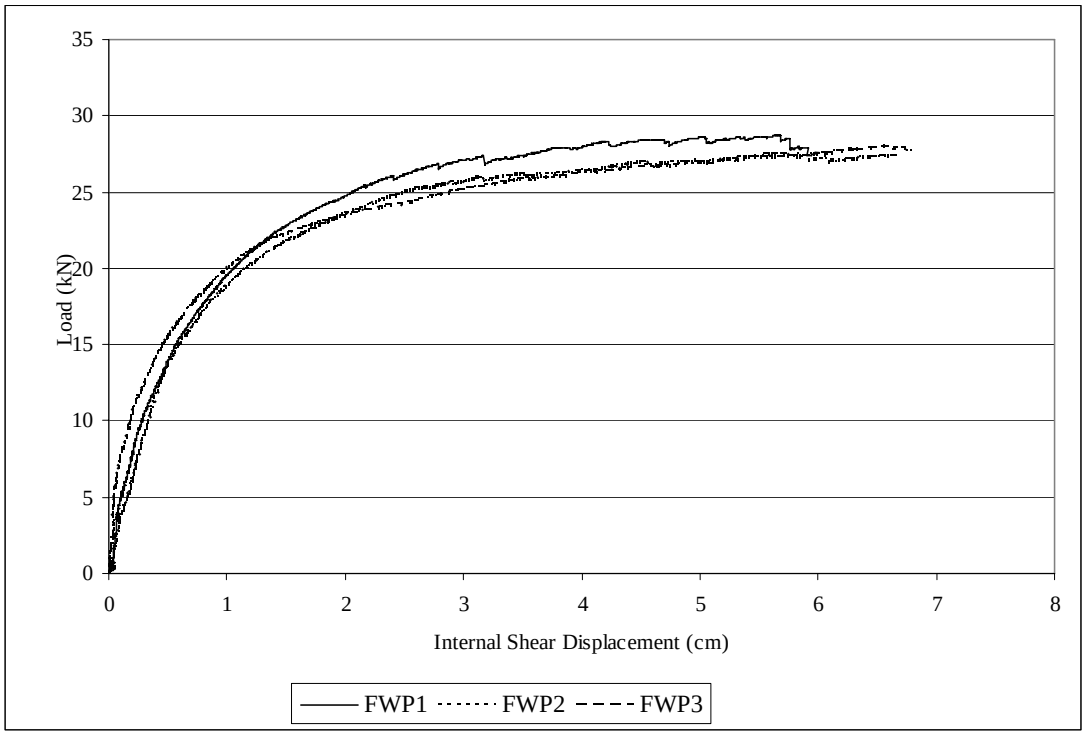

Figure 2.7 Internal shear displacements for walls with flatwise girts and WPC skirtboards.

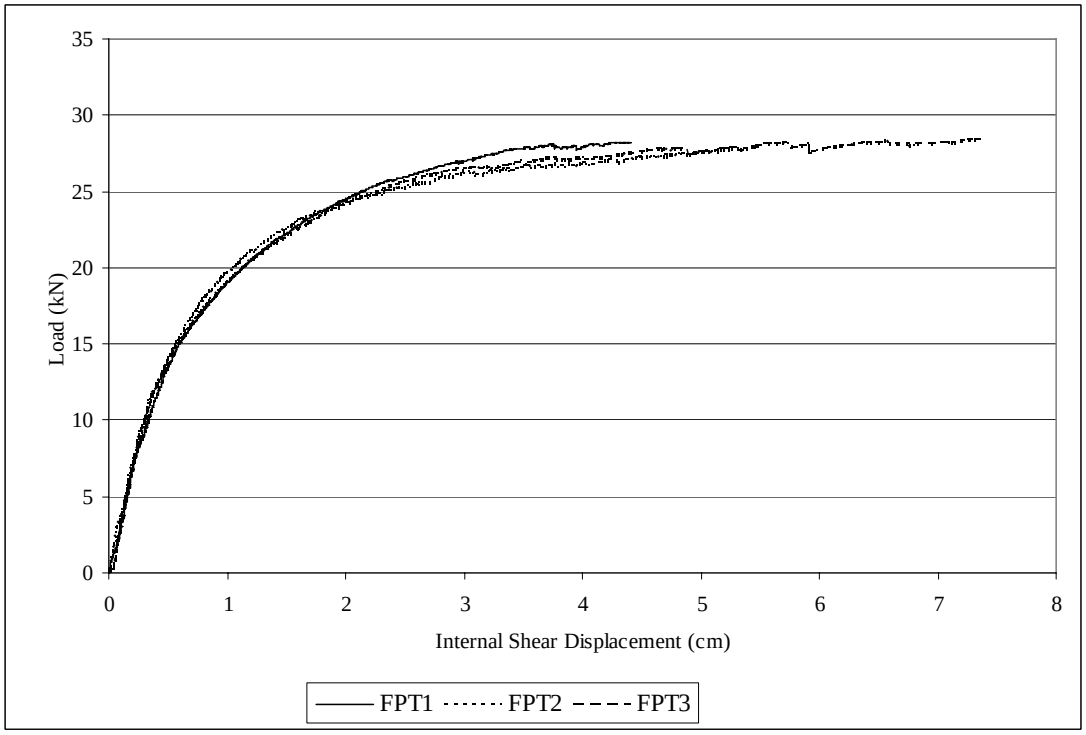

Figure 2.8 Internal shear displacements of walls with flatwise girts and PPT skirtboards.

LIST OF TABLES

Table 2.1 Mechanical Properties of WPC Used

Property	ASD Value (kPa)
Flexural stress	1725
Tension	1725
Modulus of Elasticity	6.895×10^5
Compression parallel to grain	3790
Compression perpendicular to grain	4300
Shear	1380

Table 2.2 Results of Each Wall Test

Wall	Internal Shear Displacement at		Internal Shear Stiffness	Ultimate Shear Strength	Design Strength
	Max Load	Design Load	G_{int}	S_u	2.5 Safety Factor
	cm	cm	kN/m	kN/m	kN/m
EPT1	6.0107	0.2999	3862.3	7.92	3.17
EPT2	4.1580	0.3102	3646.9	7.73	3.09
EPT3	5.2795	0.3237	3410.0	7.55	3.02
EWP1	4.4653	0.2899	4047.7	8.02	3.21
EWP2	6.0917	0.3870	2851.6	7.54	3.02
EWP3	4.0302	0.4286	2438.0	7.14	2.86
FPT1	4.4102	0.3875	2915.4	7.72	3.09
FPT2	5.4709	0.3451	3238.8	7.63	3.05
FPT3	7.3684	0.3683	3090.5	7.78	3.11
FWP1	5.6702	0.3537	3247.9	7.85	3.14
FWP2	7.1234	0.2296	4884.9	7.49	3.00
FWP3	6.6560	0.3683	2977.2	7.67	3.07

Table 2.3 Average Properties of Each Wall Configuration

Wall Type	Internal Shear Stiffness G_{int}		Ultimate Shear Strength S_u		Design Strength 2.5 Safety Factor
	Average kN/m	COV	Average kN/m	COV	kN/m
EPT	3639.7	5.1%	7.73	2.0%	3.09
EWP	3112.4	21.9%	7.57	4.7%	3.03
FPT	3081.6	4.3%	7.71	0.8%	3.08
FWP	3703.3	22.8%	7.67	1.9%	3.07

CHAPTER 3

Monotonic and Reverse Cyclic Testing of Light-Frame Shear Walls with Alternate Sill Plate Materials and Holdown Methods

ABSTRACT

A construction challenge is presented by the use of holdowns in timber structures since they can be expensive and time consuming to install. Another challenge is to identify alternatives to preservative pressure treated (PPT) lumber for sill plates. The use of a wood-plastic composite (WPC) sill plate can replace the use of holdowns with an easier system to install due to its flexibility to be extruded into different shapes and by also eliminating the need for PPT lumber. Two such alternatives to holdowns are presented, one with a thicker WPC sill plate and light-gage steel gusset plates and the other with a WPC sill plate that is continuously embedded into the concrete foundation. Both alternatives were found to have slightly higher shear wall strengths as compared to conventionally framed shear walls with holdowns.

INTRODUCTION

Historically, two methods of designing light-frame shear walls have been used. One method is given in the International Residential Code (IRC) as prescriptive guidelines. These prescriptions call out spacing of anchor bolts, nailing schedules, and bracing. The second method is given in the International Building Code (IBC) which requires “engineered walls.” These give specific strengths based upon nailing schedules and material used. The IBC also requires some means of restraining uplift either by the dead load of the building or holdown hardware.

A limiting factor of the IRC braced shear walls is their ability to resist the uplift caused by the horizontal forces acting on the wall. Without requiring holdowns, the sheathing nails and

the sill plate are required to resist the uplift, which results in brittle failures (Mahaney 2002). Unfortunately, holdowns can be costly and difficult to install, so while requiring them in every IRC shear wall would improve the performance and safety of the structure, it may not be economical.

This study examines two alternatives to holdowns in comparison to prescriptive IRC shear walls, specifically in the maximum cyclic shear strength, stiffness, and ductility. The first alternative is a simple solution of adding a light-gauge metal gusset plate to the corner of the walls to help transfer uplift loads from the framing to a wood-plastic composite (WPC) sill plate. The WPC sill plate is thicker than conventional dimension lumber so localized bending moments are better resisted and fastener edge distances are increased. The second alternative is the use of an "L"-shaped sill plate that is continuously embedded into the concrete foundation. This method does not utilize any form of holdown or anchor bolts and it is anticipated that the intermediate studs would help resist the uplifting forces.

Both alternatives replace the PPT sill plate with a WPC, which resists decay without the use of preservative chemicals. Copper rich preservative chemicals can increase corrosion in the metal fasteners and weaken the system. Also the incising of the lumber required for the penetration of the chemicals weakens the sill plate in flexure (both cross grain and parallel to grain), which are primary failure mechanisms for walls without holdowns. By using a WPC, these problems can potentially be mitigated.

LITERATURE REVIEW

Many in the design community considered wood-frame buildings resistant to seismic loadings due to being highly redundant and ductile; however, the Northridge Earthquake on

January 17, 1994 raised some serious questions. Over 95% of all fatalities in the Northridge Earthquake and one-half of all property damage occurred in wood-frame structures (Mahaney 2002). These events caused national concern because 90% of all residences in the United States are wood-frame (Bracci 1996). Sill plates were one of the major problems found in site visits after the Northridge Earthquake (Day 1996).

In light of the Northridge Earthquake, the Consortium of Universities for Research in Earthquake Engineering (CUREE) created the CUREE-Caltech Woodframe Project due to the obvious need for more understanding of earthquake phenomenon and wood structures. The CUREE researchers identified that sill plates are a weak link in wood-frame shear walls. The general failure of sill plates was identified as splitting due to cross-grain bending and twisting. The bending of the sill plate occurred because of the uplift due to the overturning of the wall. The twisting occurred because of the inherit eccentricity of the anchor bolts and sheathing (Mahaney 2002).

The uplift forces on the sill plate can cause a significant decrease in the capacity of the walls. In the CUREE testing, walls with different aspect ratios were tested to evaluate the effect of the uplift forces on capacity. Walls with an aspect ratio of 1:1 and no holdowns held only one-fourth the amount as a wall with an aspect ratio of 1:4 (Mahaney 2002.) One possible solution to resist uplift forces is placing holdowns on the wall (Mahaney 2002). When holdowns are added, the walls' capacity can increase by a factor of three (Cobeen 2004). However, holdowns are often complex to install and require time consuming tasks for those working on the concrete and framing of the structure. It is estimated that nearly 22% of all holdowns are misinstalled (Lebeda 2005). Even with properly installed holdowns, the ultimate failure of the sill plate is brittle. In

fact, the large diameter bolts used in holdowns can cause a Mode I yielding (AF&PA 2005) and cause the sill plate to split (Bracci 1996).

One way to reduce splitting of the sill plate due to twisting and tension perpendicular to grain is to increase the thickness of the sill plates to 6.35 cm; however, these can still exhibit brittle failure (Bracci 1996). Another solution is to increase the size of the washers on the anchor bolts to increase the bearing area to offset the eccentricity on the sill plates. Increasing from a 5 cm square washer to a 6.35 cm washer can improve the capacity of the walls by as much as 20% (Mahaney 2002). Similarly, sill plates confined with steel straps or similar devices can resist higher loads and have the added advantage of maintaining 75% of the walls' maximum strength after the sill plate has split (Bracci 1996).

Another possible solution purposed by Duchateau (2005) is to create a WPC sill plate that is continuously embedded into the concrete foundation. Also, WPCs resist decay, which was a considerable cause of failure in the North Ridge Earthquake (Day 1996). Generally, the bottom 15 cm of woodframe walls is susceptible to decay (Duchateau 2005). A WPC sill plate together with proper house wraps and flashing should adequately protect this area. Additionally, an embedded WPC sill plate would provide an insect barrier and reduce air infiltration.

Duchateau (2005) proposed a continuously embedded sill plate after testing a variety of WPC sill plates. The most successful was a stranded section shown in Figure 3.1, with pockets to facilitate connection of the studs to the sill plate. Steel dowels were inserted through the end stud and cavity of the WPC sill plate to create a holdown. The primary failure modes were in flexure of the sill plate and tension perpendicular to the extrusion. Duchateau commented that these failures might be prevented if the WPC sill plate were continuously embedded into the concrete to remove flexure and to reduce the tension forces by sharing them with intermediate

studs. The continuously embedded sill plate examined herein is to test Duchateu's hypothesis. The other sill plate in this study is a simpler, non-continuously embedded system that has a sill plate without pockets for studs, and the anchor bolts closer to the end studs to reduce flexure of the sill plate. Steel gusset plates were used to help transfer the uplift forces from the stud into the sill plate.

METHODS AND MATERIALS

Materials

The sill plates were made with a WPC formulation of 55% pine flour, 41% polyethylene, and 4% lubricant by weight. The lubricant was TPW Structural 104. The WPC was extruded with a Milacron TC86 with Barrel-Zones 1 through 4 and the screws at 171° C. All three die zones were 177° C. The WPC was extruded as a 14 cm by 2.5 cm deck-board, which was subsequently melt-bonded to form the final 13.7 cm by 14 cm sill plates.

Due to the high cost of manufacturing an extrusion die, two different prototype sill plates were created with a melt bonding process explained in the Methods Section. Eventually, these shapes could be achieved through extrusion without the need for melt bonding. One section was a 3 ply (6.8 cm) member that served as a thicker traditional sill plate made out of WPC. The other sill plate was 6 plies and was cut into the shape shown in Figure 3.2 with a table saw. This shape was designed to be imbedded into a concrete foundation to serve as a continuous attachment. The asymmetric cross section was chosen to avoid weakening the portion of the concrete nearest the outside face of the foundation.

The load path for the continuously embedded sill plate has to transfer the uplift forces from the studs to the sill plate and finally to the concrete foundation. To achieve this load path

for a proof of concept, the sill plate for the continuous foundation was attached to 16 gauge (0.15 cm) A569 sheet metal which attached the sill plate to the studs (Figure 3.2). The metal was to approximate Duchateu's system and provide load transfer from the studs to the sill plate. Such a heavy gauge metal was chosen to force the failure to be in the WPC. The metal was attached to the WPC with 11, 1.9 cm long by 0.3 cm wide sheet metal screws. Holes were predrilled into the WPC with a diameter of 0.32 cm to facilitate screw insertion. The layout of these screws on the sheet metal is shown in Figure 3.3a.

The concrete foundations were constructed to be 30.5 cm wide and tall by 3.35 m long. The concrete was a 6 sack concrete with a max aggregate size of 1.9 cm and 4 to 7% air entrapment. The mixture represented a typical residential mix for the local area. It was reinforced with two #4 rebars at mid-height of the foundation. The continuous foundation was further reinforced with five #3 rebars bent into an inverted "U" shape to reinforce the concrete edge undergoing tension to resist sill plate uplift. This reinforcing was placed 15 cm from the edge of the foundations and 30 cm o.c. with the top of the inverted "U" being 30 cm in length.

For the non-continuous foundations, three 1.59 cm diameter holes were drilled into the concrete to post-install anchor bolts. Simpson RFB #4X10 retrofit bolts were then installed with Simpson's SETPAC-EZ high strength epoxy. The anchor bolts had a diameter of 1.3 cm and a length of 25.4 cm and were embedded 15.3 cm into the concrete. The end anchor bolts were placed 11.4 cm from the end of each wall. This placement created a 1.3 cm gap between the edge of the 5 cm square washer and the double end stud. Similarly, the middle anchor bolt was placed so that a 1.3 cm gap would exist between the washer and the center stud.

The walls were constructed with Douglas-fir 3.8 x 14 cm lumber. Stud grade was used for the studs and No. 2 or better were used for the top plates. The studs were spaced 40.6 cm o.c.

with a double stud at the ends of each wall. The sheathing was 11 mm thick and was nailed 15.2 cm o.c. around the edges and 30.5 cm o.c. in the middle of the panels. The nails used for framing the studs were galvanized 10d (3.3x89 mm) box nails. A total of six nails were used to tie the double end studs together. Three rows of two nails were used, and the rows were 61 cm apart. Similarly, two nails were driven into the top of each stud through the bottom piece of the top plate. Three nails were driven at each stud to tie the two pieces of the top plates together. The lumber had an average moisture content of 13% (dry basis) at the time of construction as measured by a capacitance meter. The average moisture content at the time of testing was 7.9%.

The control walls had an incised PPT sill plate that was Hem-fir graded as No. 2 or better 3.8 cm thick. The studs were nailed through the sill plate and into the end grain of the studs. The thick, non-continuously embedded WPC sill plate also had a 61 by 61 cm right-triangle steel gusset plate attached to the end of each wall. The steel was galvanized 24 gauge attached to the outside of the sheathing. The attachment of the metal consisted of two nails equally spaced between the sheathing nails that were 15.2 cm o.c. The nailing configuration is shown in Figure 3.3. The nails used for the sheathing of both the control walls and the walls with thickened sill plates and their gusset plates were bright 8d (3.3x64 mm) common nails. All the nails were driven with a pneumatic nail gun without predrilling.

The walls with a continuously embedded sill plate had 16 gauge sheet metal attached to each stud with nails equally spaced between the sheathing nails. The plates extended 61 cm up from concrete foundation. The nails were 8d (3.9x76 mm) common nails and were used for both the attachment of the metal and the sheathing.

Methods

The melt bonding process consisted of placing two deck-boards 46 cm under two Fostoria 135kW infrared heat lamps. The surface temperature of the WPC was monitored using a Fisher Scientific IR thermometer. After approximately 15 minutes, the WPC reached 140° C. One of the deck-boards was then flipped on top of the other, and both were placed in a hydraulic press. A jig was made to improve the accuracy of aligning the two boards and to prevent a board from slipping under the pressure applied by the press. The press was displacement controlled to the thickness of the combined deck-boards minus 0.8 mm for the WPC to squeeze out of the sides. Generally, the press read a pressure of 518 kPa. The press was held for five minutes at the determined thickness before releasing the boards.

The melt bonding of multi-ply deck-boards followed the same procedure, only more time was needed to heat the WPC to 145° C. A higher temperature was needed to offset the conductive heat losses to the material behind the heated surface.

All shear walls were tested according to Method C, the CUREE protocol, in ASTM E 2126 (2007). A monotonic test was performed on walls with the thickened sill plate and the continuous embedment to find the appropriate Δ, the reference deformation for cyclic tests upon which the displacement of each cycle is calculated. The Δ for the control walls was estimated from previous experience. The Δ of the walls without holdowns, steel gusset plates, and continuously embedded sill plate were 1.56 cm, 2.16 cm, and 2.5 cm respectively. All tests were performed at frequency of 0.5 Hz.

Four resistance potentiometers were used to measure displacements. One was attached to the top plate of the wall to measure the global displacement. Another was attached to the sill

plate to measure rigid body translation with respect to the concrete foundation. The other two measured the uplift of the end studs.

A 50 kN double acting hydraulic actuator with a 100 kN load cell applied the load to the top of the walls. The actuator was attached to the wall with a pin connection to prevent moment from being transferred into the load cell. The weight of the actuator was not applied to the top of the walls – this was accomplished by extending the top plate of each wall by 61 cm with a double stud at the end to hold up the actuator. Out-of-plane lateral displacement was prevented by attaching rollers that glided on fins attached to the testing frame. The concrete foundations were attached to the laboratory strongfloor with four 3.8 cm diameter threaded rods that went through vertical conduits left in the foundations and were screwed into the floor. For the walls with continuously embedded sill plates, bracing was added to the end of the concrete foundation to prevent possible translation.

RESULTS AND DISCUSSION

Definition of Calculated Values

The results calculated for the cyclic wall tests followed ASTM E 2126-07 procedures; however, some discussion is needed as to how these values were calculated. Nearly all walls failed in a brittle manner, so the failure was defined as the peak displacement instead of degradation to 80% of peak. The brittle failure of the walls also caused one direction of the hysteresis to undergo a peak that the other direction did not. Since the actuator first pushed on the wall, which was recorded as a negative displacement and load, most of the walls failed at a negative peak. The exceptions to this were the walls with a triangular gusset plates because the nail withdrawal governed their failure, which was less sensitive to direction and less brittle.

The value of the maximum load resisted is defined as the largest load the wall resisted in either direction. The shear strength, displacement at peak, and ductility are all based on the stronger direction of the wall. The stiffness is based upon the average of both directions since initial stiffness is not influenced by the ultimate load or displacement.

The values were also calculated to reduce the effect of the translation during testing. The feedback of the actuator was used to measure the global displacement of the walls during testing; however, for the walls with the gusset plates, the concrete foundation slid as much as plus or minus 0.7 cm. Unfortunately, this was not noticed until testing was completed and this component of translation could not be isolated and removed. The walls with a continuously embedded foundation had the concrete braced to remove any translation. The displacement of the concrete was then measured and found to be zero. Similarly, the values given have been modified to account for the translation of the sill plate relative to the concrete, which was subtracted from displacements given so that only shear and rotation are presented.

Since the walls had a concrete foundation, the sheathing of the walls would bear on the concrete when loaded. This effect caused the center of rotation of the panels to not be in the center of the panel. While this difference probably more accurately mimics a wall in the field, many wall tests do not have any foundations that influence the rotation of the panels. This difference most likely gives these walls a higher stiffness than if they were mounted on a steel channel.

Values for the hysteretic energy absorbed or damping could not be accurately calculated with the test data. Unfortunately, the equipment used had a maximum data acquisition rate of eight points per second, and since the walls were tested at a rate of 0.5 Hz, only eight points were

recorded over a typical movement of 2 cm at the peak load. Such few points make calculating energy inaccurate.

Failure Modes

The control walls with a PPT sill plate and no holdowns failed in a similar manner described by Mahaney (2002). The sill plate split due to cross-grain bending along the line of the anchor bolts. The split was sudden and brittle, and once split, the wall could not resist load and would translate back and forth with the actuator. Figure 3.4 shows a typical split of the sill plate. The nails that attached the sheathing to the sill plate at the corners also underwent withdrawal from the sheathing as shown in Figure 3.5. Little damage was visually apparent outside of the two corners.

The monotonic test of the wall with a triangular gusset plate failed with the nails withdrawing from the WPC sill plate as shown in Figure 3.6. No damage was observable on the gusset plates, which suggests that an even lighter gage sheet metal might be adequate. The gusset plate also prevented the two primary failure mechanisms of the sheathing nails in the control wall. It prevented the nails from pulling through or tearing out the OSB. Significant bending was seen in the sill plate and separation of the melt bonds was seen during testing as shown in Figures 3.7 and 3.8 respectively.

The cyclic tests with the gusset plates failed in a similar manner. The nails ultimately failed in withdraw from the WPC. Replacing the smooth nails with threaded nails would likely improve the system. While not the primary failure mechanism, the corner of the OSB broke off at 5 to 7 cm. from the edge due to compressing against the concrete. The gusset plate similarly

buckled from the compression. An example is shown in Figure 3.9. The nails on the shared stud of the panels also ripped out of the OSB.

The monotonic test for the wall with continuously embedded WPC sill plate showed the potential of such a system. During testing it was noted that the double top plate was bending and causing the actuator to push upwards on the wall. To help prevent this effect, a restraining chain was wrapped over the top plate at the connection to the actuator. Unfortunately, this prevented uplift from occurring on the wall as shown in Figure 3.10. However, it also prevented the major failure of the cyclic tests: delamination of the melt bond. Since a true commercial product would not be melt bonded, but simply extruded into the correct shape, the plane of weakness might not govern. The monotonic results suggest the capability of such a system, which is nearly twice the strength of the other walls tested as summarized in Tables 3.1 and 3.2.

The cyclic tests with the embedded WPC sill plate failed primarily at the melt bond. Since the quality of the melt bond was variable, the performance of these walls was variable as well. The first cyclic wall was considerably stronger, and the reason was easily seen when viewing the foundation after failure. The WPC failed at a combination of the melt bond and extruded WPC as shown in Figure 3.11. It was estimated that 80% of the failure was material failure and 20% was melt bond failure. The second cyclic wall was the weakest and the melt bond failure was estimated at nearly 80%. The third wall was in between the other two with an estimated 60% failure due to the melt bond.

Since the melt bond caused premature failures, the expected failures of nail-shear around the metal sheet or nail withdrawal did not happen. In fact, very little damage existed outside of the sill plate.

Comparison of Wall Types

The walls with the gusset plates were the easiest alternative to install and have the largest ultimate displacement; however, due to the translation of the concrete foundation for that series of tests, this value is questionable. If the speculated value of 0.7 cm of translation is subtracted from the ultimate displacement of the walls with gusset plates, the value becomes nearly the same as that of the control walls. The walls with the continuously embedded sill plate showed the smallest ultimate displacement. This result is likely due to the lack of rotational translation undergone by these walls. The configuration required less rotation before resisting uplift, so smaller drift was expected.

The shear walls with embedded WPC sill plates were the stiffest, but while such a sill plate would likely be stiffer than the others, the sheet metal likely caused the greatest contribution. The metal caused fixity to the bottom of the studs which caused bending rather than racking of the studs. While such foundations studied previously by Duchateau would obviously cause some fixity to exist, it is doubtful that it would be as much as caused by the steel in this experiment. The significant improvements made by both the triangular gusset plate and the continuously embedded sill plate can be seen in Table 3.2 which has the individual and average values of the three cyclic walls including the outlier second, continuously embedded wall.

On average, the walls with the gusset plates are shown to be the strongest, but this superior strength is likely due only to the premature failure of the melt bond of the continuously embedded sill plates. This explanation is presumed due to the continuously embedded wall with the best melt bonding being significantly stronger than the walls with the gusset plates. In fact, if the continuously embedded wall with the failure being nearly completely melt bond is considered an outlier, the embedded walls are stronger on average by 13% or 1.5 kN/m.

In comparison to the capacity of walls with holdowns as given in Special Design Provisions for Wind and Seismic Supplement (AF&PA 2005) Table 4.3A, the walls with the steel gusset plates and the continuously embedment were 7% stronger. Duchateau (2005) tested walls with a thickened sill plate that had cavities which allowed steel rods to be placed through the end studs and act as a holdown. Duchateau's walls were about the same strength as the walls tested in this study; her walls were only stronger by 1.7%. However, the walls with gusset plates were 61% stiffer, and the walls with continuous embedment were 145% stiffer than the walls in Duchateau's study.

CONCLUSION

This study tested an alternative to the use of PPT lumber as a sill plate by using WPC. Since WPCs can be extruded into shapes the might reduce the labor or improve the properties of shear walls, two alternatives were tested to remove holdowns. One alternative was a 6.8 cm thick, solid WPC sill plate with two 24 gauge steel gusset plates. The other alternative was a sill plate that was continuously embedded into the concrete.

Both studied alternatives have been shown to be viable options to resist the uplifting forces on shear walls. The continuously embedded walls were the stiffest and strongest if the wall test with the weakest melt bond is ignored, but showed the smallest ultimate displacement and ductility. The triangular gusset plate system would clearly be the easiest to install and inspect. Both wall types had an average strength of approximately 11.5 kN/m, which is nearly double the strength of a light-frame shear wall without holdowns and a 7% increase in capacity compared to walls with holdowns.

The walls with gusset plates showed a similar improvement of strength to a holdown, yet their installation is not as complex. The gusset plates did not fail but the nails withdrew from the WPC sill plate, and the gusset plate prevented nail pullout or tearing of the OSB. Further study of gusset plates with fasteners better capable of resisting withdrawal should be conducted. Similarly, a “U”-shaped, double sided gusset plate that wraps under the sill plate might also prevent this primary failure mechanism by more directly transferring the load into the anchor bolt.

Unfortunately the poor melt bonding of the continuously embedded sill plates caused premature failures that would not exist in a commercial product; however, this study does show the potential of such a system. If a better method of melt bonding is developed or directly extruding the desired shape is possible, further studies should provide better results. Until then, the melt bond remains a difficulty of testing these types of walls.

Literature Cited

American Forest and Paper Association, Inc (AF&PA). (2005). "Lateral force resisting systems." *Special design provisions for Wind and Seismic*, AF&PA, Washington, DC,11-28.

AF&PA. (2005). "Appendix I: Yield limit equations for connections." *National design specification for wood construction ASD/LRFD*, AF&PA, Washington, DC, 158.

American Society for Testing and Materials (ASTM). (2007). "Standard Test Methods for cyclic (reversed) load test for shear resistance of vertical elements of the lateral force resisting systems for buildings" *ASTM E 2126-07a*, West Conshohocken, PA: ASTM.

Cobeen, Kelly, Russell, James, and Dolan, Daniel. J. (2004) "Interconnection of elements" *Recommendations for earthquake resistance in design and construction of woodframe buildings*, CUREE, Richmond, CA, 131-142.

Day, Robert W. (1996). "Performance of single family house foundations during northridge earthquake." *Practice periodical on structural design and construction*, 1(2), 85-88.

Duchateau, Kristi A. (2005). "Structural design and performance of composite wall-foundation connector elements." MS Thesis, Washington State University, Pullman, WA.

Englund, Karl, and Wolcott, Michael P. (2005). "Lamination of wood plastic composites by utilizing an infrared heating apparatus." *Commercialization of navy wood composites: final report*, Washington State University, Pullman, WA, 1-8.

Lebeda, Dana. J et al. (2005). "Effect of hold-down misplacement on strength and stiffness of wood shear walls." *Practice periodical on structural design and construction*, 10(2), 79-87.

Mahaney, James. A., and Kehoe, Brian. E. (2002). "Anchorage of Wood-frame Buildings: Laboratory Testing Report (CUREE Publications No. W-14)," CUREE, Richmond, CA.

Notation

The following symbols are used in this paper

Δ_e = the deformation at 0.4 Peak

Δ_u = the ultimate deformation

Δ_{yield} =P_{yield} / K_e

A = area under the envelope curve

COV = coefficient of variation

Ductility = Δ_{yield} / Δ_u

K_e = 0.4 Peak / Δ_e

P_{yield} = $\left(\Delta_u - \sqrt{\Delta_u^2 - \frac{2A}{K_e}}\right)K_e$

LIST OF FIGURES

Figure 3.1 Duchateu's (2005) WPC sill plate section with steel dowels running through the cavities of the sill plate and into studs which are pocketed in the sill plate.

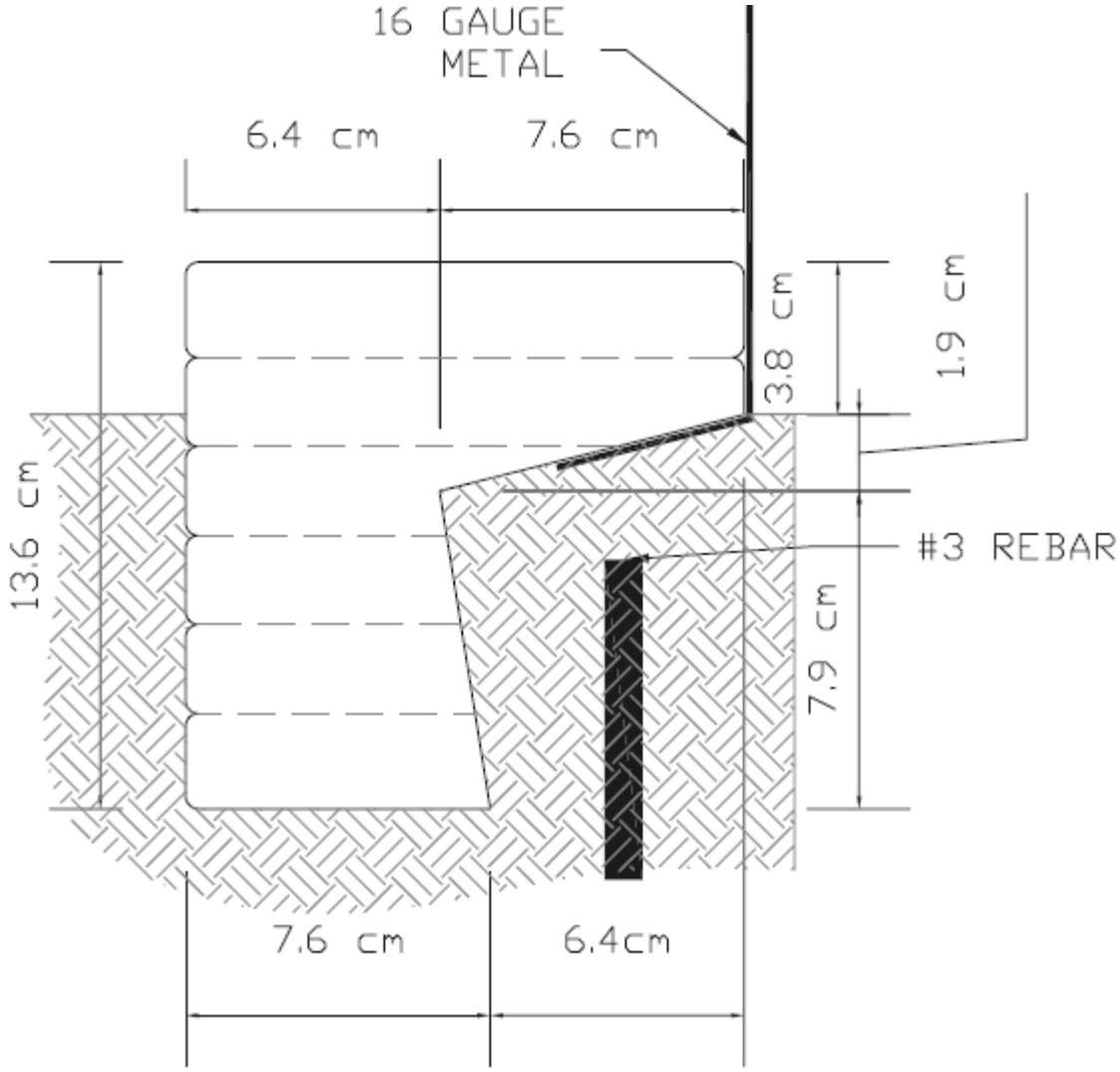

Figure 3.2 Section of the continuously embedded sill plate. Dashed lines show locations of melt bonding.

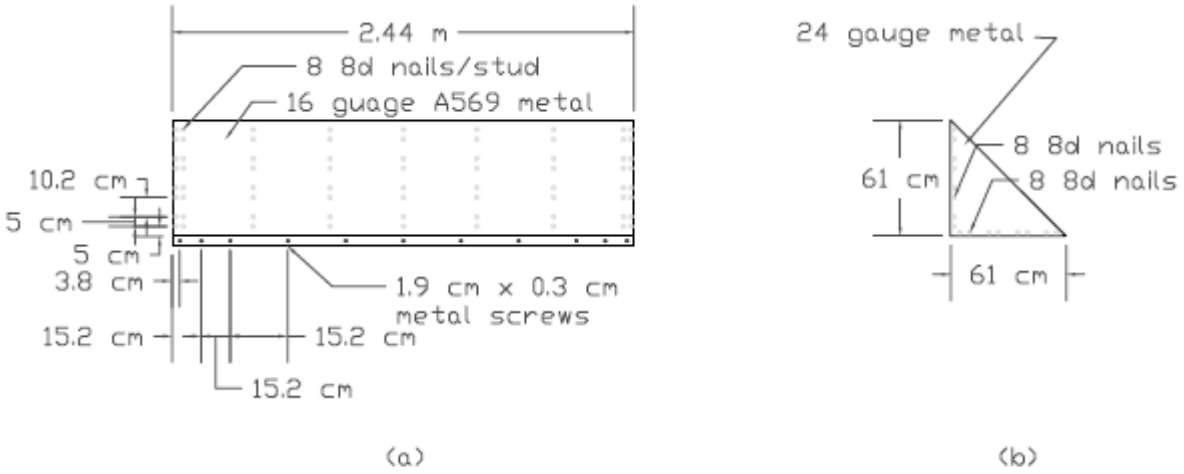

Figure 3.3a and 3.3b Layout of sheet metal and fasteners for the (a) continuously embedded sill plates and the (b) guest plates

Figure 3.4 Splitting of PPT Hem-fir sill plate without holdowns

Figure 3.5 Nail head pull-through from sheathing of walls without holdowns

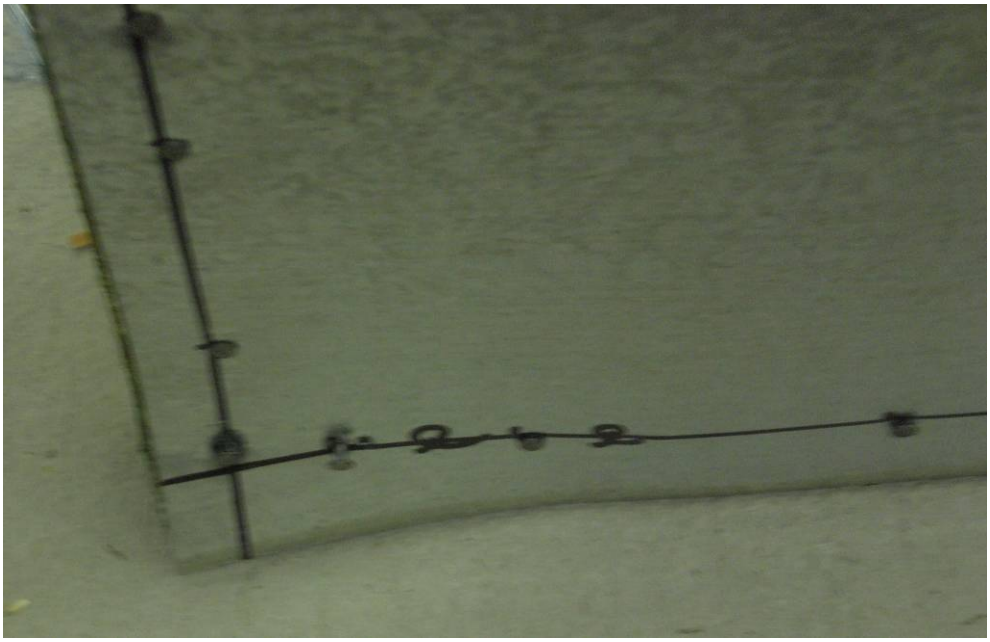

Figure 3.6 Nail withdrawal of triangular gusset plate at corner of wall

Figure 3.7 Bending of thickened WPC sill plate with triangular gusset plates (attached to other side)

Figure 3.8 Separation of the sill plate along the melt bond

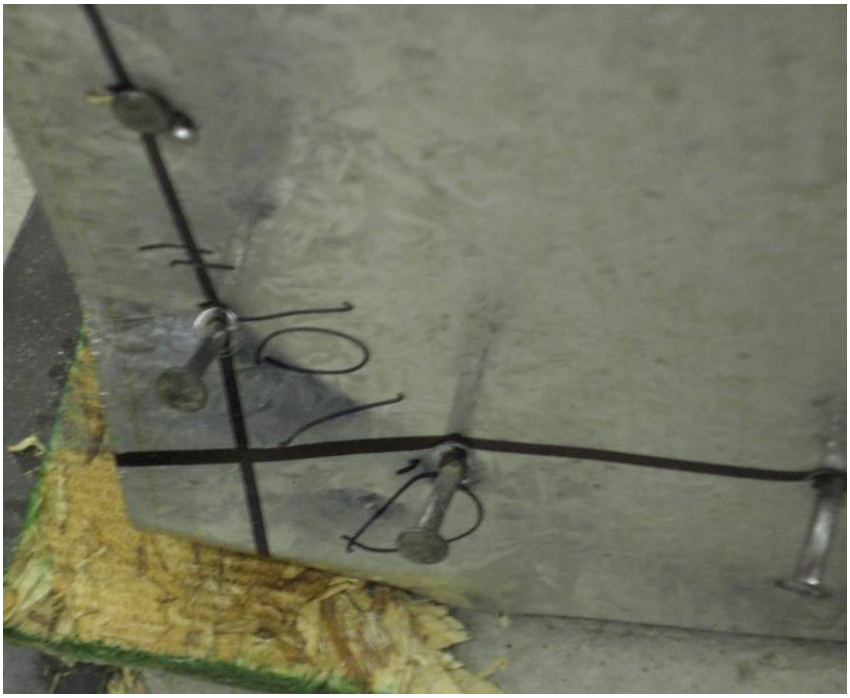

Figure 3.9 Buckling of metal gusset plate and damage of OSB at corner of wall

Figure 3.10 Restraint of uplift forces on the monotonic wall with a continuously embedded sill plate

Figure 3.11 Failure of the first continuously embedded wall. Light colored area is WPC failure and the dark colored area is melt bond failure.

LIST OF TABLES

Table 3.1 Monotonic test results

Monotonic Wall Type	Max Load	Shear Strength	K_e
	kN	kN/m	kN/cm
Continuous Foundation	53	21.7	14.72
Triangle Gusset	19	7.7	15.92

Table 3.2 Reverse cyclic test results

Wall Type	Iteration Number	Shear Strength kN/m	Ductility Value	P_{yield} kN	Δ_u cm	K_e kN/cm
Continuous Foundation	1	14.3	2.8	30	2.410	32.05
	2	8.3	1.6	31	0.846	30.09
	3	11.4	1.7	22	1.420	26.00
	Average	11.4	2.0	27	1.559	29.38
	COV	22%	27%	15%	41%	9%
Triangle Gusset	1	10.7	2.5	18	2.695	19.02
	2	12.5	2.6	25	3.327	17.88
	3	11.3	3.7	23	4.450	21.28
	Average	11.5	2.9	22	3.491	19.39
	COV	6%	19%	13%	21%	7%
Control	1	5.9	6.5	12	4.260	18.60
	2	5.6	2.3	12	1.481	18.50
	Average	5.8	4.4	12	2.870	18.6
	COV	2%	48%	0%	48%	0%

CHAPTER 4

Summary and Conclusions

This paper includes the research done on substituting a PPT foundation element with a WPC. Sometimes this substitution was direct as was done with the skirtboards of post-frame walls, but it also includes the use of WPC in a more creative way to eliminate holdowns in light-frame walls. Both studies showed that WPC can be used structurally as a foundation element with either similar or improved results of traditional PPT lumber and hardware. In fact, the post-frame study showed that after an ANOVA testing that there were no statistically significant differences between flatwise and edgewise girt orientations or between PPT and WPC skirtboards. Similarly, the light-frame section showed that WPC with alternatives to holdowns can be used and improve upon a similar wall with a PPT sill plate and holdowns by 7%.

Future studies should improve upon the finding of this study. Specifically, studies into the use of WPC as either the bottom section or all of the post in post-frame buildings could cause the removal of PPT lumber from such structures altogether. Similarly, research into the use of threaded nails with the steel gusset plates could improve upon the capacity of that alternative, and an improved method of melt bonding the WPC will clearly improve upon the results of the continuously embedded sill plates.

Appendix “A” gives hysteretic graphs and the data points for the backbone curve of each light-frame wall.

APPENDIX A – LIGHT-FRAME WALL RESULTS

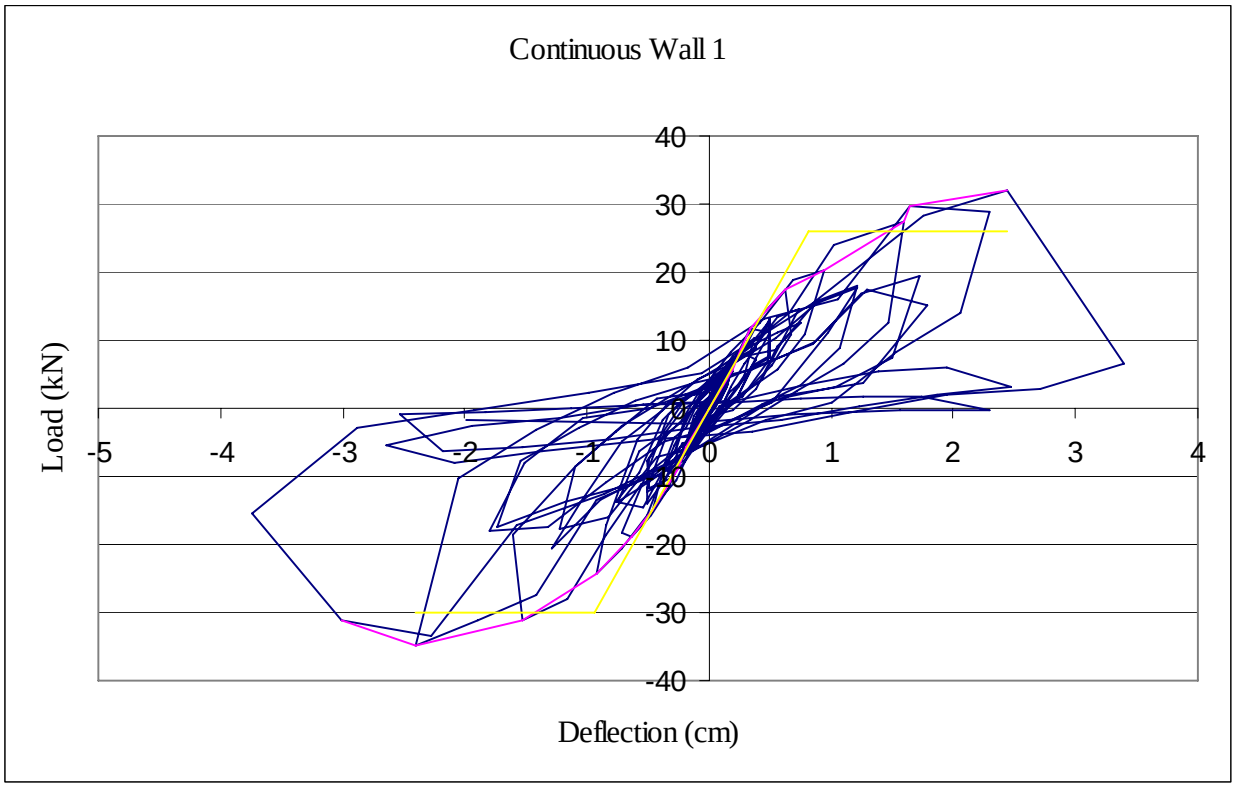

Load (kN)	Δ (cm)
-31.255	-3.007
-34.962	-2.410
-31.234	-1.534
-24.394	-0.922
-18.847	-0.630
-14.818	-0.467
-8.734	-0.249
-5.735	-0.185
5.798	0.193
8.565	0.249
11.670	0.343
17.316	0.622
20.261	0.942
27.531	1.595
29.810	1.648
31.926	2.446
20.261	0.942
27.531	1.595
29.810	1.648
31.926	2.446

Figure 1A Hysteresis and envelope data of first wall with a continuously embedded WPC sill plate.

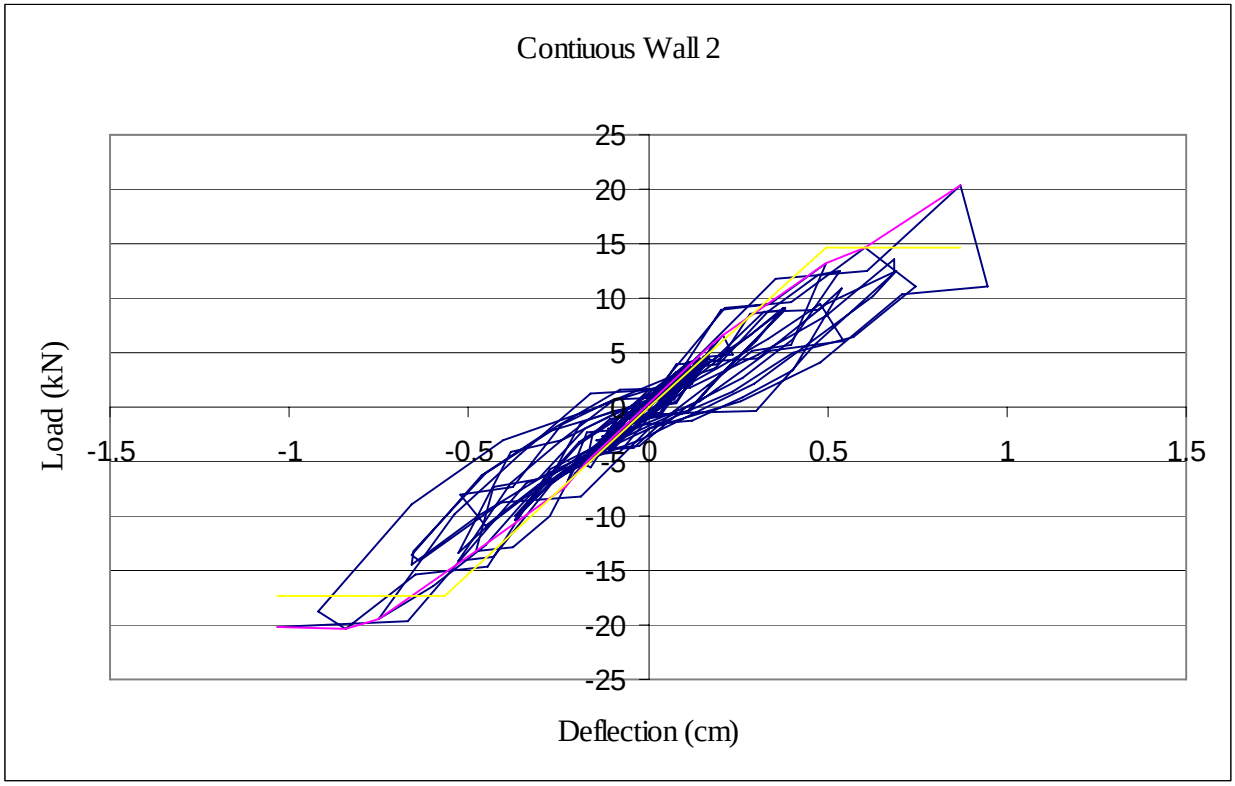

Load (kN)	Δ (cm)
-20.2658	-1.0312
-20.3485	-0.8458
-19.4249	-0.7518
-13.1789	-0.4826
-7.3400	-0.2311
-4.9860	-0.1727
5.9060	0.1829
6.6137	0.2083
13.1718	0.4978
14.5945	0.6045
20.3313	0.8687

Figure 2A Hysteresis and envelope data of second wall with a continuously embedded WPC sill plate.

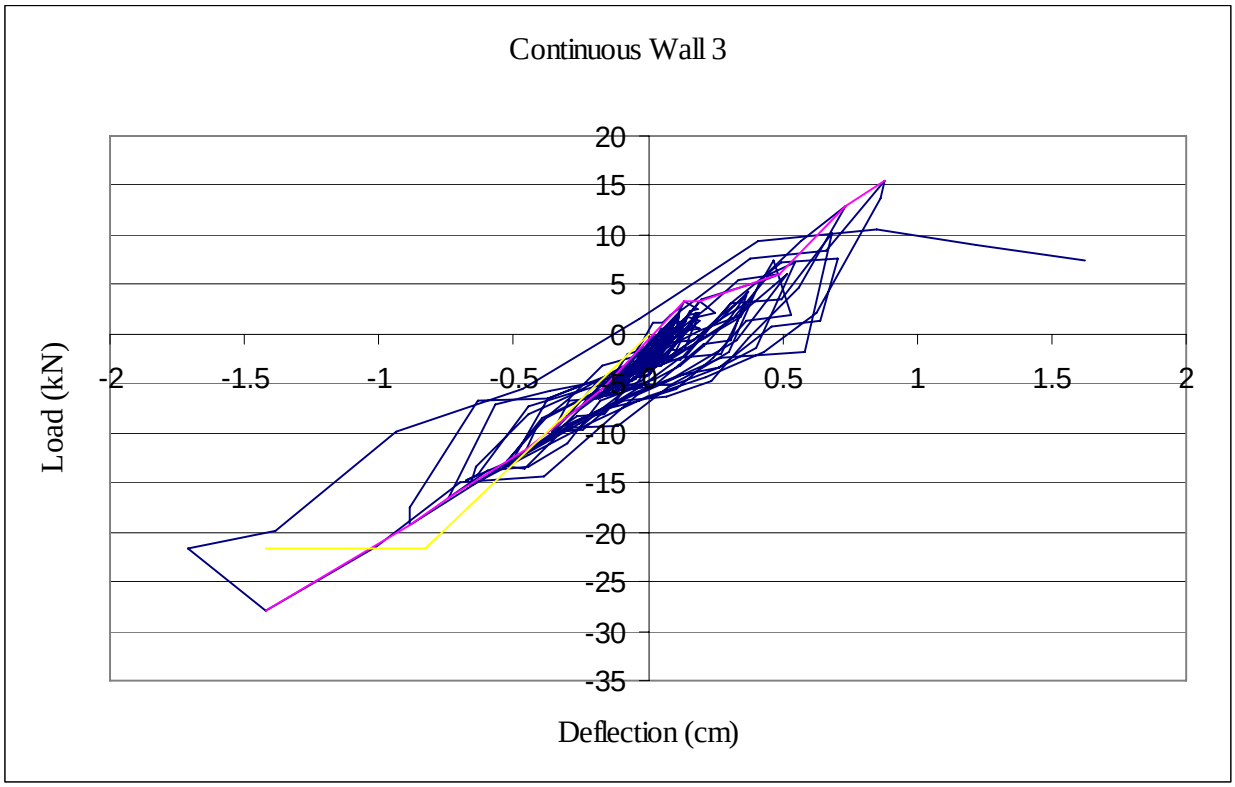

Load (kN)	Δ (cm)
-27.887	-1.420
-19.289	-0.886
-16.462	-0.742
-11.593	-0.450
-7.113	-0.239
-5.460	-0.168
3.318	0.132
3.272	0.193
6.006	0.485
12.899	0.734
15.563	0.876

Figure 3A Hysteresis and envelope data of third wall with a continuously embedded WPC sill plate.

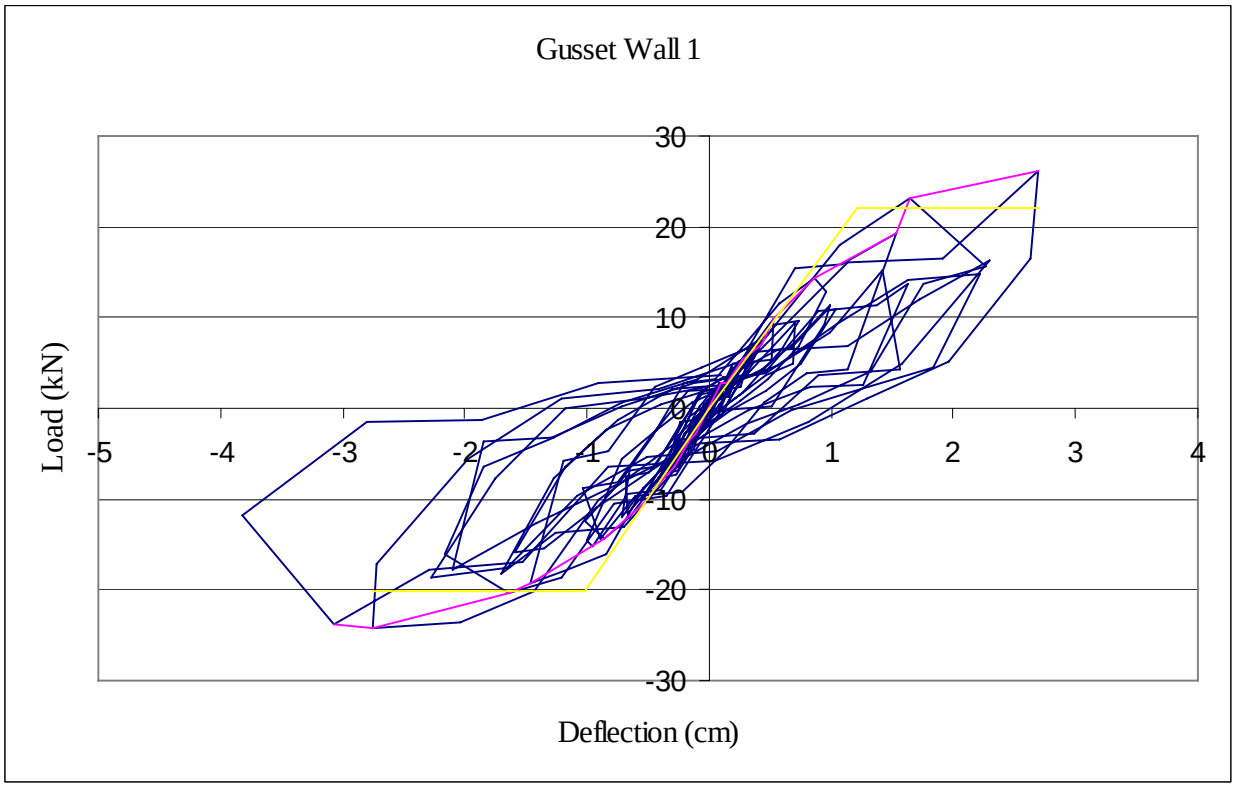

Load (kN)	Δ (cm)
-23.679	-3.066
-24.168	-2.751
-20.332	-1.646
-19.391	-1.463
-14.299	-0.853
-9.971	-0.508
-8.599	-0.427
-6.490	-0.287
-3.487	-0.152
-2.793	-0.117
2.680	0.097
2.813	0.152
5.332	0.267
6.979	0.437
9.875	0.528
14.444	0.861
19.366	1.527
23.236	1.646
26.196	2.695

Figure 4A Hysteresis and envelope data of first wall with a thickened WPC sill plate and steel gusset plate.

Load (kN)	Δ (cm)
-24.025	-4.122
-24.058	-3.475
-23.136	-2.591
-23.585	-1.880
-18.011	-1.382
-17.358	-0.965
-10.638	-0.566
-8.264	-0.394
-5.725	-0.262
-3.396	-0.152
-2.537	-0.107
2.385	0.112
2.512	0.157
5.045	0.264
7.679	0.414
9.635	0.572
13.563	0.848
18.505	1.433
25.190	2.220
27.620	2.543
30.427	3.327
27.917	4.105

Figure 5A Hysteresis and envelope data of second wall with a thickened WPC sill plate and steel gusset plate.

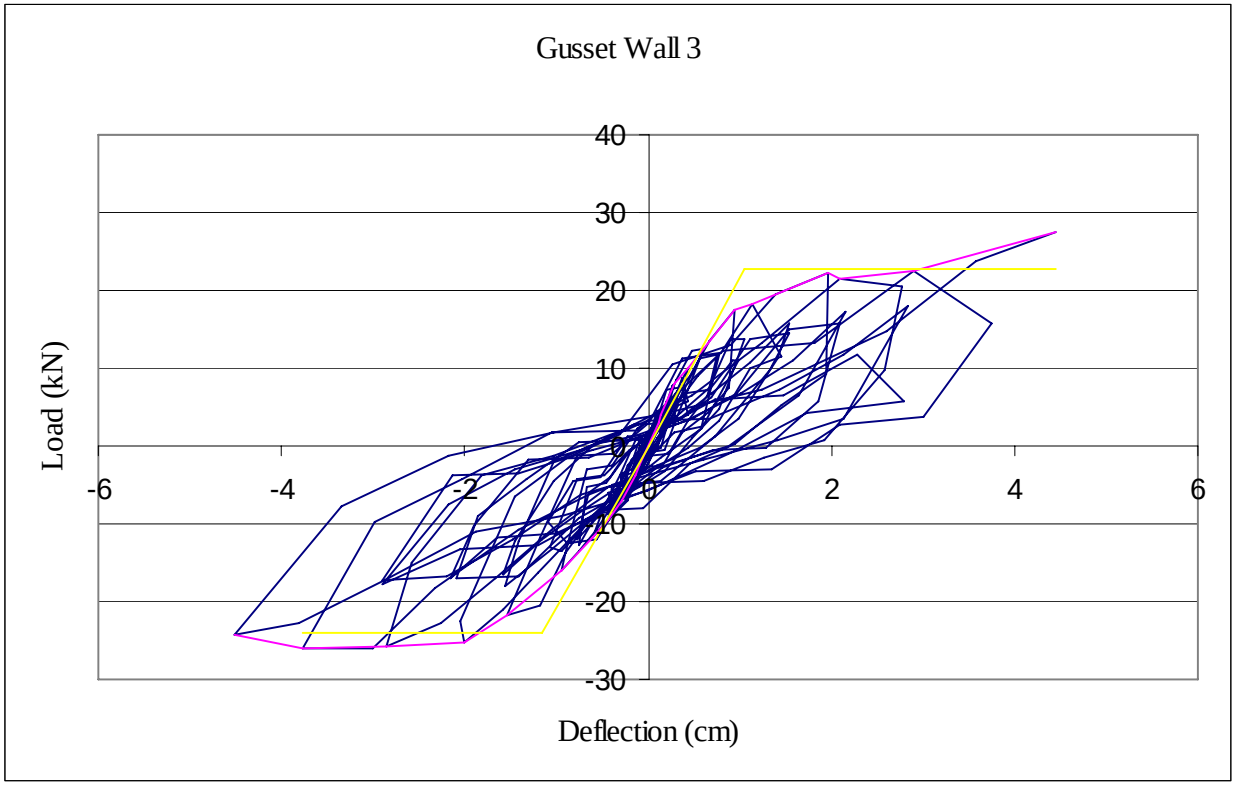

Load (kN)	Δ (cm)
-24.316	-4.509
-26.123	-3.780
-25.818	-2.865
-25.197	-2.014
-21.829	-1.539
-15.923	-0.955
-11.845	-0.599
-9.486	-0.427
-7.104	-0.287
-3.862	-0.145
-2.592	-0.099
2.930	0.107
4.053	0.145
7.899	0.279
10.041	0.439
12.403	0.615
17.438	0.947
18.173	1.128
22.303	1.956
21.614	2.093
22.515	2.893
27.488	4.450

Figure 6A Hysteresis and envelope data of third wall with a thickened WPC sill plate and steel gusset plate.

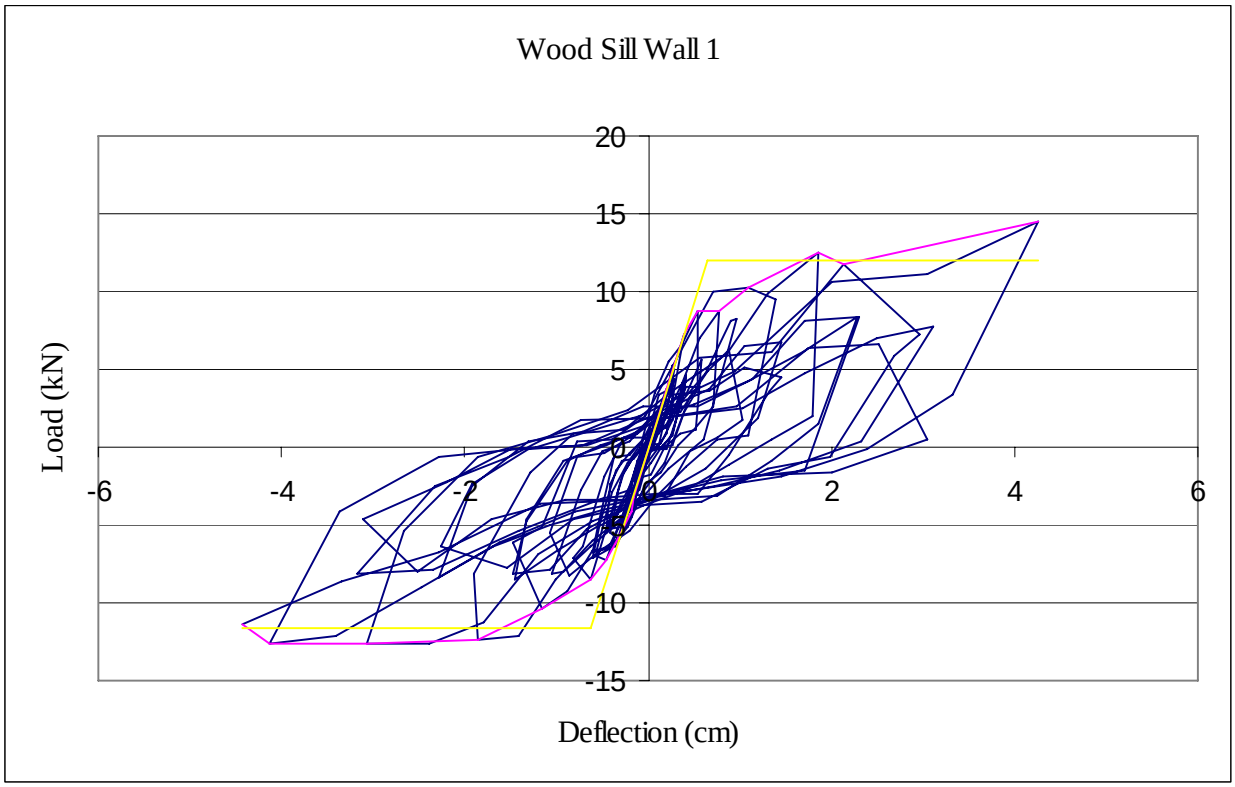

Load (kN)	Δ (cm)
-11.313	-4.430
-12.679	-4.140
-12.661	-3.076
-12.326	-1.854
-10.354	-1.161
-8.483	-0.632
-7.260	-0.447
-5.825	-0.333
-4.071	-0.188
-3.283	-0.155
2.863	0.155
3.746	0.201
7.237	0.394
8.721	0.533
8.717	0.767
10.214	1.092
12.498	1.854
11.764	2.141
14.447	4.260

Figure 7A Hysteresis and envelope data of first wall with a PPT sill plate and no holdowns.

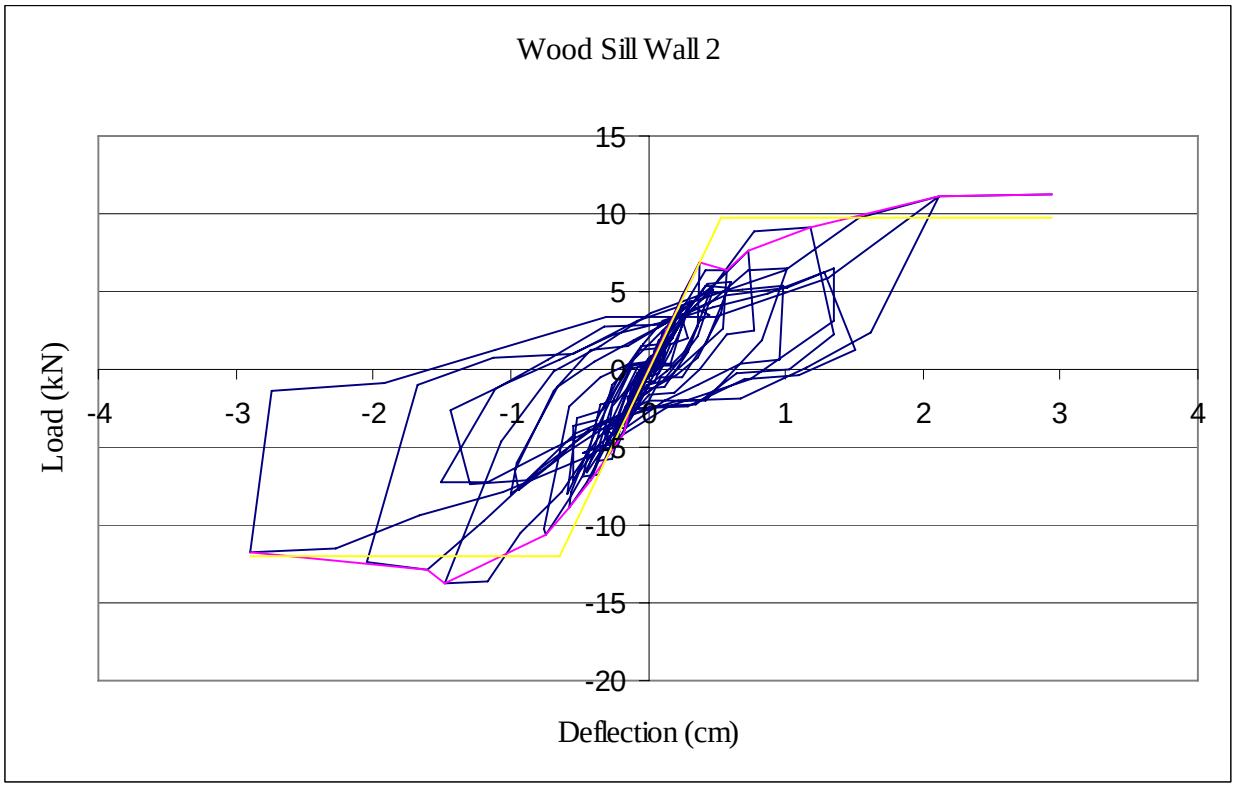

Load (kN)	Δ (cm)
-11.773	-2.896
-12.920	-1.610
-13.760	-1.481
-10.563	-0.742
-8.822	-0.566
-7.076	-0.414
-4.077	-0.183
-2.602	-0.140
2.497	0.137
3.736	0.208
6.932	0.371
6.424	0.574
7.596	0.726
9.140	1.184
11.142	2.113
11.299	2.944

Figure 8A Hysteresis and envelope data of second wall with a PPT sill plate and no holdowns.